JOURNAL OF MATERIALS SCIENCE 26 (1991) 127–134

The polymorphs of zirconia: phase abundance and crystal structure by Rietveld analysis of neutron and X-ray diffraction data

C. J. HOWARD
Australian Nuclear Science and Technology Organisation, Lucas Heights Research Laboratories, PMB 1, Menai, NSW2234, Australia

R. J. HILL*
Mineralogisches Institut, Universität Würzburg, Am Hubland D-8700 Würzburg, FRG

Rietveld analysis of neutron and X-ray powder diffraction data has been used to obtain the crystallinity and relative abundances of cubic (22 at% Y), tetragonal (5.8 at% Y), and monoclinic zirconia in synthetic binary and ternary mixtures of the pure phases. The stabilized cubic and tetragonal forms are shown to be 94(2) and 96(2)% crystalline, respectively, but no amorphous material was detected in the chemically pure monoclinic phase. In both stabilized polymorphs, the yttrium atoms randomly substitute into the zirconium site, with a charge-compensating proportion of vacancies on the oxygen atom site. In this near worst-case situation of very similar cubic and tetragonal unit cell dimensions, the phase abundances determined by Rietveld analysis of neutron data are very accurate and superior to those determined by integrated-intensity methods of analysis. For X-ray data, the accuracy is diminished by the presence of extinction, and by uncertainty in the definition of the peak shape of the cubic phase due to the absence of intense high-angle reflections and the resultant dependence on strongly overlapping low-angle data.

1. Introduction

Accurate measurement of the relative abundances of the cubic (C), tetragonal (T) and monoclinic (M) polymorphs of zirconia is of considerable importance in attempts to understand, and thereby manipulate, the physical and mechanical properties of zirconia-based ceramics [1–3]. This is especially true for the so-called partially stabilized zirconia (PSZ). Although other phases can be produced under special conditions (e.g. orthorhombic [4] and δ-phase [5]), this material consists largely of binary or ternary mixtures of the C, T and M polymorphs, and displays enhanced strength and toughness due to the martensitic transformation of T to M under certain critical conditions of size and stress [6].

The significant industrial and technological importance of these ceramics has resulted in many attempts (mostly using X-ray diffraction) to provide a reliable and universal method for the determination of phase abundance information. Most of these attempts are applications of what has become known as the "polymorph method" [7], which is based on the measured intensities of selected reflections in a single diffraction scan. In this paper, we demonstrate the use of the Rietveld method [8] for phase analysis of mixtures of C-, T- and M-zirconias. The Rietveld method, like the polymorph method, yields phase abundances from the analysis of a single diffraction pattern, but the analysis makes use of the whole diffraction pattern rather than a few reflections in it. We find, as expected, that the Rietveld method is more powerful, in that it can provide information of phase abundances even in cases (e.g. ternary mixtures) which are intractable by the polymorph method.

2. An account of the polymorph method

The polymorph method is closely related to the "direct comparison method" for quantitative phase analysis [9], first applied for measuring the retained austenite in steel [10]. It is based on the proportionality, which holds within a given diffraction pattern under certain idealized conditions [9, 11],

$$I_{ip} \propto (R_{ip}/\rho_p)m_p \qquad (1)$$

where I_{ip} is the integrated intensity of the ith reflection in the pth phase, R_{ip} a quantity depending on the phase p and the particular reflection i which can be calculated from crystal structure information‡, ρ_p the theoretical density of phase p and m_p is the mass of phase p in the mixture, which is assumed homogeneous. The method makes use of integrated intensities of selected reflections, sums of intensities over groups of reflections, and ultimately the ratios of intensities (or sums of intensities) as described in detail below.

In the $(C + M)$ and $(T + M)$ binary systems, the

*On leave from: CSIRO Mineral Products, POB 124, Port Melbourne, Victoria 3207, Australia

‡In the notation of Hill and Howard [11], $R_{ip} = N_{cp}^2 J_{ip} L_{ip} |F_{ip}|^2$.

0022–2461/91 $03.00 + .12

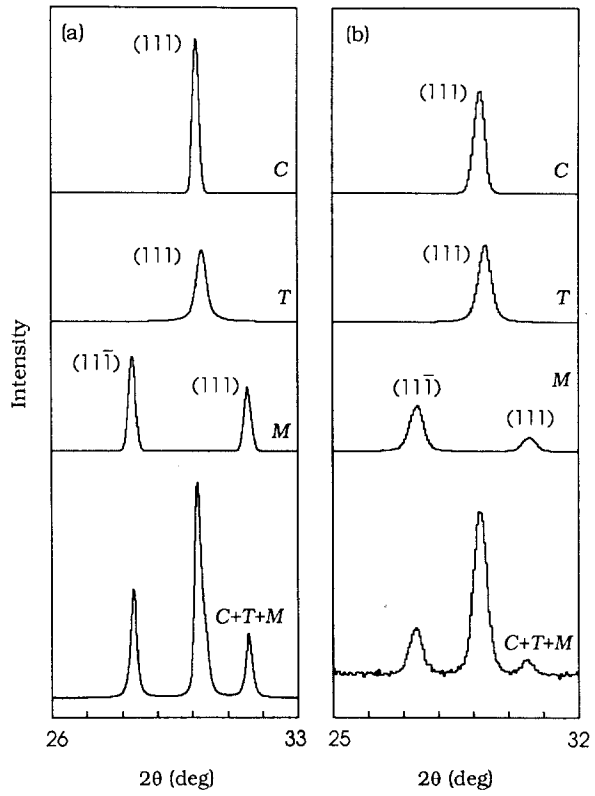

Figure 1 The set of {111} peaks from the individual component phases (calculated), and the total diffraction pattern (observed) from a 1:1:1 by weight mixture of *C*-, *T*- and *M*-zirconia. The plots are in (a) for CuKα X-rays and in (b) for neutrons of wavelength 0.15 nm. The observed pattern in the neutron case is a segment of the pattern shown in full in Fig. 3.

reflections measured are the {1 1 1} peaks around 30°2θ (for CuKα radiation), and the ratio

$$X_M = \frac{I(111)_M + I(11\bar{1})_M}{I(111)_M + I(11\bar{1})_M + I(111)_{C,T}} \quad (2)$$

is used in the analysis [7,12,13]. Note that in this, and the following equations, the *T* has been referred to the face-centred unit cell to simplify comparisons with the corresponding *C* cell. From Equation 1, the weight fraction of monoclinic is

$$W_M = \frac{PX_M}{1 + (P - 1)X_M} \quad (3)$$

where

$$P = \frac{R(111)_{C,T}}{R(111)_M + R(11\bar{1})_M} \frac{\rho_M}{\rho_{C,T}} \quad (4)$$

The simplest form of the polymorph method [12–14] made use of the approximation $P \approx 1$ so the intensity ratio X_M gave the weight fraction W_M directly. The method has been improved by elaborating the calculation of *P*, incorporating the Lorentz-polarization factors [7], and the structure factors for the different polymorphs [15–17]. The *C* and *T* polymorphs almost always contain another cation (usually yttrium, calcium or magnesium) added to render them stable at room temperature, and the detailed effects of this stabilizer have also been taken into account in the structure factor calculation [18,19]. An alternative approach is the experimental determination of *P* by the least squares fit of (3) to X_M against W_M as determined in calibration experiments [16, 20]. The use of profile-fitting techniques to determine the integrated intensities [16, 18, 21, 22] has resulted in considerable improvements in the precision and accuracy of the method.

When *C* and *T* are present together, in either the (*C* + *T*) binary or the (*C* + *T* + *M*) ternary systems, the {111} peaks from *C* and *T* are not resolved. This is clear from Fig. 1, which shows the {111} peaks in X-ray and neutron diffraction patterns from a mixture comprising *C*, *T* and *M* in equal weights. Although the *C* and *T* cannot be individually determined from these peaks, the monoclinic fraction may still be obtained from Equations 2 and 3, taking for $I(111)_{C,T}$ the total intensity of the unresolved *C* and *T*, and for *P* the average value of P_C and P_T weighted according to the (assumed or approximate) relative amounts of *C* and *T* in the mixture.

Some success has been achieved in discriminating between *C* and *T* using the {200} reflections around 35° 2θ [19] but, since the resolution is generally better at higher diffraction angles, the {400} peaks around a 2θ angle of 73° are usually preferred. The {400} peaks in X-ray and neutron diffraction patterns from a mixture of equal weights of *C* and *T* are shown in Fig. 2. The appropriate intensity ratio is [6, 23]

$$X_T = \frac{I(004)_T + I(400)_T}{I(004)_T + I(400)_T + I(400)_C} \quad (5)$$

and the weight fraction of *T* is given by

$$W_T = \frac{QX_T}{1 + (Q - 1)X_T} \quad (6)$$

where

$$Q = \frac{R(400)_C}{R(004)_T + R(400)_T} \frac{\rho_T}{\rho_C} \quad (7)$$

In the (*C* + *T* + *M*) system, the presence of interfering monoclinic peaks (when *M* is present in substantial amounts) makes a determination of *T* and *C* by this approach very difficult to impossible [19].

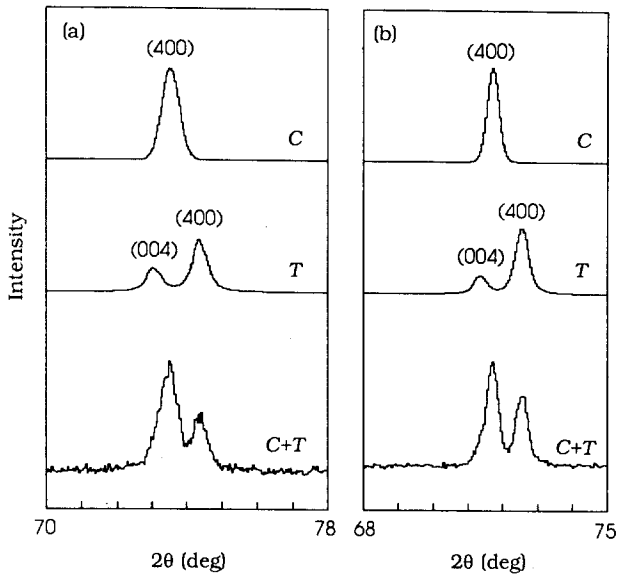

Figure 2 The set of {400} peaks from the individual component phases (calculated), and the total diffraction pattern (observed) from a 1:1 by weight mixture of *C*- and *T*-zirconia. The plots are in (a) for CuKα X-rays and in (b) for neutrons of wavelength 0.15 nm.

In its simpler forms, the polymorph method provides a rapid and fairly reliable determination of M in a mixture with C or T, or both*. The polymorph method determination of C and T in the $(C + T)$ system is more difficult, and in the $(C + T + M)$ system usually intractable. The accuracy has sometimes been found wanting, and the method in its more developed form requires sophisticated curve-fitting procedures, and structure factor calculations based on realistic crystal structure models for the stabilized C and T phases. Even then, the results depend on the measured intensities of very few (typically three) often severely overlapping peaks, and these may be affected by problems such as extinction, micro-absorption, and preferred orientation.

3. The Rietveld method for quantitative phase analysis

Application of the Rietveld whole-pattern fitting method [8, 24] offers a solution to many of the limitations of earlier methods of phase analysis for the ZrO_2 polymorphs, documented above. In particular:

(i) The crystal structure and diffraction profile parameters of each phase can be refined together in the anaylsis of the observed pattern, so that the structural and chemical details of the particular components in the mixture are adjusted automatically and dynamically.

(ii) All reflections in the powder diffraction pattern are explicitly included in the analysis. This helps overcome the problem of overlapping reflections, and makes the results less prone to error from the effects of extinction and preferred orientation, which tend to affect only a few strong reflections.

(iii) The background is more accurately determined by fitting a polynomial over the entire pattern.

(iv) The relative abundances of the phases in a mixture are a simple function of their relative scale factors as determined in the Rietveld analysis so that Equations 2 to 7 are not required. The expression for the weight fraction of phase p, which is also derived from Equation 1 [11], is

$$W_p = \frac{S_p (ZMV)_p}{\sum_i S_i (ZMV)_i} . \quad (8)$$

where S, Z, M and V are, respectively, the Rietveld scale factor, the number of formula units per unit cell, the mass of the formula unit, and the unit cell volume.

(v) The absolute weight fractions of the components in a mixture may be obtained if an internal standard is added in a known proportion.

Details of the successful application of the Rietveld method (Equation 8) for quantitative analysis have been described for minerals [11, 25–27], batteries [25], and PSZ materials [28]. While the method is equally applicable for X-ray or neutron data, the use of neutrons has the particular advantage of providing very low absorption coefficients, so that the deleterious effects of microabsorption, the bane of X-ray work, are virtually eliminated, and bulky (i.e., non surface-specific) samples can be analysed directly [28].

In the present study, Rietveld analysis of neutron and X-ray powder diffraction data is used to obtain the relative abundances of the ZrO_2 polymorphs in various binary and ternary mixtures of the pure phases, and the results are compared with those obtained using traditional integrated-intensity methods, as embodied in Equations 2 to 7. Attention is focused on binary mixtures of Y-stabilized C and T zirconia since this is the most demanding of any quantitative analysis system. As a preliminary to the analysis of the polymorph mixtures, the crystallinity of each ZrO_2 phase is measured by comparison with a standard sample of corundum. Rietveld analysis of neutron data collected on the end-member C, T and M phases is also undertaken to characterize their crystal structures and to determine the location and abundance of the stabilizer cation, where present.

4. Experimental details

4.1. Sample preparation

The samples used for data collection were all essentially single-phase powders prepared from zirconia containing the natural abundance of hafnium (about 2 wt %). The M sample was a commercial unstabilized ZrO_2 product from Z-Tech Corporation (grade S994 EF-Premium), obtained from zircon by a plasma dissociation process. The T sample was stabilized with yttria and was prepared by coprecipitation (SY-ULTRA from Z-Tech). Crystal structure refinement of this sample using neutron powder diffraction data (see below) yielded a composition of $Zr_{0.98}Y_{0.02}O_{1.99}$. The C sample was also prepared by coprecipitation using yttrium as the stabilizing cation, but in this case, the precipitate was calcined at 1200 °C for 48 h; shorter annealing times produced C phases with a bimodal distribution of unit cell dimensions, probably reflecting components with different mean yttrium content. The product had a composition of $Zr_{0.78}Y_{0.22}O_{1.89}$ from the crystal structure refinement. The corundum used as an internal standard for the measurements of ZrO_2 crystallinity was a sample of "Linde C" (1.0 μm) that had been well characterized in earlier trials [11]. A summary of the crystallography of these phases is provided in Table I.

The phases were combined to give the various binary and ternary mixtures indicated in Table I (weighing to at least four significant figures), each with a volume of approximately 10 cm^3, as required for neutron diffraction. The mixtures were homogenised by hand grinding in a pestle and mortar.

4.2. Diffraction data collection

4.2.1. Neutrons

Samples of the pure phases (with the exception of corundum) and the mixtures shown in Table I, were loaded into 16 × 50 mm V cans and mounted on the eight-counter, fixed-wavelength, high-resolution, powder diffractometer (HRPD) at the Australian Nuclear

*The case in which the mixture also contains orthorhombic zirconia and the δ-phase has recently been discussed by C. J. Howard and E. H. Kisi, *J. Amer. Ceram. Soc.* **73** (1990) 10.

TABLE I Summary of phase, sample and neutron powder data refinements

	Cubic-ZrO_2	Tetragonal-ZrO_2	Monoclinic-ZrO_2	Corundum[a]
Formula	$Zr_{0.78}Y_{0.22}O_{1.89}$	$Zr_{0.98}Y_{0.02}O_{1.99}$	ZrO_2	Al_2O_3
Space group	$Fm3m$	$P4_2/nmc$	$P2_1/c$	$R\bar{3}c$
ZMV[b]	67.039	16.828	70.422	156.034
Max. step int. (cnts)[c]	2480	1230	470	780
No. reflections	18	55	366	36
No. str. params[d]	5	6	16	6
No. profile params	8	8	8	8
R_{wp} (%)[e]	8.17	5.63	6.37	6.71
G of F[e]	3.45	1.74	2.13	1.22
R_B(%)[e]	1.83	1.42	2.26	0.88
Impurity phase (wt %)[f]	1.2(2)T-ZrO_2	0.8(2)M-ZrO_2	Nil	Nil
Crystal size (nm)	396(33)	47(1)	65(2)	1000(50)
R.m.s. strain (%)[g]	0.146(2)	0.127(3)	0.096(3)	0.0
Crystallinity (%)[h]	94.2(20)	95.8(22)	100.0(28)	100.0
Mixtures examined				
C-ZrO_2/Al_2O_3	1:1			
T-ZrO_2/Al_2O_3	1:1			
M-ZrO_2/Al_2O_3	1:1			
C-ZrO_2/T-ZrO_2	1:3 1:1 3:1			
$C/T/M$ ZrO_2	1:1:1			

[a]Refinement details published in [11].
[b]Product of Z, the number of formula units in the unit cell, M, the mass of the formula unit (in atomic mass units), and V, the unit cell volume (in nm^3)
[c]Represents the average value collected on each of eight detectors.
[d]Includes atomic positional, occupancy (where stabilized) and displacement parameters, and unit cell dimensions. For C-ZrO_2, one of the parameters is associated with oxygen atom displacement parallel to ⟨111⟩.
[e]Standard Rietveld refinement agreement index [32].
[f]Numbers in parenthesis here and elsewhere represent the estimated standard deviation in terms of the least significant figure to the left.
[g]Root-mean-square strain based on an assumed Gaussian distribution [24, 28].
[h]From phase analysis of data from binary mixtures with corundum (assumed to be 100% crystalline).

Science and Technology Organisation's research reactor (HIFAR) at Lucas Heights, New South Wales. This instrument (in an earlier single-counter configuration) has been described previously [29]. The data were recorded at 295 K at intervals of 0.05° from 15° to 160° 2θ, using a wavelength of 0.15 nm.

4.2.2. X-rays

Portions of the 1:1 $C:T$ and 1:1:1 $C:T:M$ mixtures used for neutron data collection were back-pressed into standard 20 × 10 mm aluminium holders and placed in a Philips Bragg-Brentano diffractometer fitted with a PW1710 automatic step-scanning system, a curved graphite diffracted-beam monochromator, and divergence and receiving slit dimensions of 1° and 0.2 mm, respectively. The diffraction patterns were recorded at 295 K with a fine focus copper tube ($\lambda = 0.154\,056$ nm for α_1, and 0.154 439 nm for α_2) using a take-off angle of 6°. Data were collected between 20° and 140° 2θ at intervals of 0.025° using step counting times of 5 and 10 sec, respectively, for the 1:1 and 1:1:1 mixtures.

4.3. Rietveld analysis

4.3.1. Neutron data

The least-squares crystal structure and profile refinements were undertaken with the multiphase Rietveld analysis program LHPM7 [24]. Details of the refinement procedure have been described elsewhere [30, 31]. Starting values for the structure parameters of the single-phase samples were taken from the results of earlier neutron powder diffraction studies of the ZrO_2 polymorphs [31] and of corundum [11]. For the mixtures, the structural parameters were held fixed at their single-phase values. The scattering lengths used for zirconium, yttrium, magnesium, aluminium and oxygen were 7.166 (modified from 7.160 to account for the presence of hafnium), 7.75, 5.375, 3.449 and 5.805 fm, respectively. Convergence was assumed to have been achieved when the parameter shifts in the final cycle of refinement were less than 10% of their associated estimated standard deviation (esd).

Values for the crystal size and strain of the single-phase samples were extracted with a procedure described elsewhere [24]. The relative abundances of the phases in the mixtures were determined from the respective Rietveld scale factors using Equation 8 and the ZMV values provided in Table I. The plot output from a Rietveld analysis of the diffraction pattern from the 1:1:1 mixture of $C:T:M$ ZrO_2 is provided in Fig. 3. Corresponding analyses were also performed using the integrated intensity (polymorph) method embodied in Equations 3 and 6; the appropriate values of the integrated intensities were taken from the raw data by curve-fitting methods.

4.3.2. X-ray data

The X-ray diffraction data were treated in a similar way to the neutron data from the mixtures; that is, the

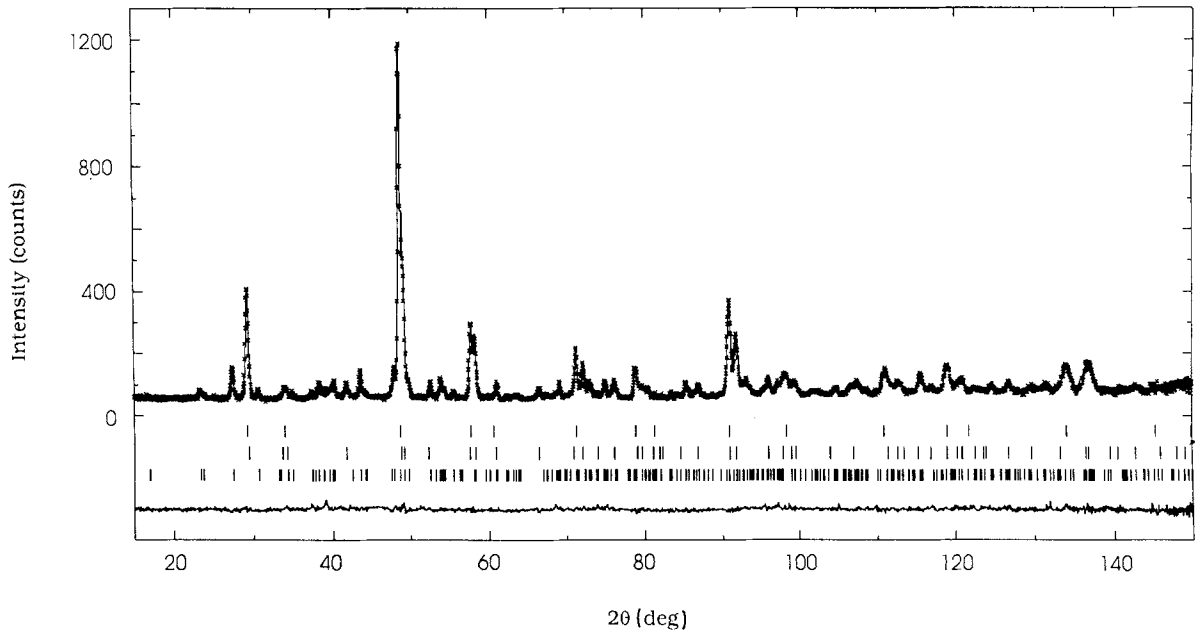

Figure 3 Plot output from Rietveld analysis of the 1:1:1 (by weight) mixture of *C*-, *T*- and *M*-zirconia ($\lambda = 0.15$ nm). Observed step-scan data are indicated by the plus signs, the calculated profile by the continuous line overlaying them, and the difference between observed and calculated by the lower curve. The positions of all Bragg reflections from the *C*, *T* and *M* polymorphs are indicated, respectively, by the three rows of markers, in descending order.

atomic coordinates, and isotropic displacement and site-occupancy parameters were held fixed at their neutron-determined values. However, in view of the significant fall-off in peak intensity with increasing diffraction angle (arising from the nature of X-ray scattering factors), the refinement was effectively restricted to the low- and medium-angle regions of the pattern where the discrimination between the *C* and *T* peaks is at its worst. As a result, it was necessary to fix the shape of the *C* peaks in all of the analyses; a pure Gaussian form was chosen in view of the large crystallite size determined for this material in the neutron data refinements (see below). Neutral atom scattering factors were used for all atoms [33], and the hafnium content of the zirconium site was specifically included in the calculations. Attempts to determine phase abundances by the polymorph method as well as the Rietveld method were made in each case.

5. Results and discussion

5.1. End-member characterization

The phase purity of the nominally single-phase ZrO_2 polymorph samples was obtained by Rietveld refinement, considering each (initially) as a mixture of *C*, *T* and *M* (corundum was known to be pure from earlier work). The resultant impurity contents are shown in Table I: the *C* sample contains 1.2(2)% *T*, the *T* sample contains 0.8(2)% *M*, and the *M* sample has no contamination within statistical error.

The crystal structure parameters obtained from the neutron refinements of the single-phase *C*, *T* and *M* samples are provided in Tables II, III and IV, respectively, where they are compared with the results of earlier work on related materials [31, 34]. These data were required in order to accurately model the crystal structures of the phases during the phase abundance determinations on the mixtures.

As in our previous studies of *C*-ZrO_2 [31], the yttrium stabilizer cation was found to substitute randomly for the zirconium atom, with a charge-compensating proportion of vacancies on the oxygen-atom site, and the oxygen atom itself displaced along the {111} direction from the ideal (0.25, 0.25, 0.25) fluorite position. There are, however, significant differences in detail between the present and earlier *C*-ZrO_2 crystal structures due to the different stabilizer cation used and its markedly different abundance in both compounds (Table II). More than 18 at % Y is required for stabilization of the *C* structure, whereas only 6 to 8 at % Mg is needed for the same function [3]. The quite dissimilar abundances, valences and sizes of yttrium and magnesium result in a much larger unit cell

TABLE II Fractional atomic coordinates, site occupancies, and isotropic displacement parameters for yttria and magnesia stabilized cubic ZrO_2

		Present work	[31]
Stabilizer cation		yttrium	magnesium
Sample form		annealed powder	sintered compact
a (nm)		0.515 55(1)	0.508 58(1)
Zr	Y/Mg occupancy (%)	22.1(19)	12.5(29)
	B(nm^2)	0.0108(2)	0.0154(3)
O	Vacancies (%)	5.5	6.3
	(x, x, x) coordinate	0.2716(7)	0.2749(6)
	B(nm^2)	0.0157(9)	0.0173(9)
Stabilizer content (at %) estimated from			
	Chemical analysis	21.1(7)	11.5(10)
	Unit cell dimensions[a]	24.9	11.8
	Unit cell dimensions[b]	24.9	9.7

[a]Using $a = 0.5105 + 0.02026$[Y] nm and $a = 0.5105 - 0.01980$ [Mg] nm [18] where [Y] and [Mg] denote the quantity (in at %) of yttrium or magnesium respectively, in the zirconium site of the crystal structure.

[b]Using $a = 0.5104 + 0.0133$ [Y] $+ 0.0088$[Y]^2 nm and $a = 0.51169 - 0.02532$ [Mg] $- 0.01176$[Mg]^2 nm [35].

TABLE III Fractional atomic coordinates, site occupancies, and isotropic displacement parameters for yttria-stabilized tetragonal ZrO_2

		Present work	[31]
Sample form		calcined powder	sintered compact
a (nm)		0.360 84(1)	0.360 55(1)
c (nm)		0.517 71(2)	0.517 97(2)
Zr	Y occupancy (%)	1.2(15)	6.5(21)
	B (nm^2)	0.0059(2)	0.0065(2)
O	Vacancies (%)	0.28	1.6
	(0.25, 0.25, z) coordinate	0.4587(2)	0.4587(2)
	B (nm^2)	0.0110(2)	0.0098(2)
Stabiliser content (atom %) estimated from:			
	Chemical analysis	5.7(5)	5.8
	Unit cell dimensions[a]	6.22	5.21

[a]Mean value from $a = 0.3592 + 0.000247[Y]$ nm and $c = 0.5195 - 0.000309[Y]$ nm [36].

dimension and a smaller displacement of the oxygen atom from the (0.25, 0.25, 0.25) position in the case of yttria-stabilization, although the percentage of charge-compensating vacancies on the oxygen site is similar in both compounds. Furthermore, the degree of r.m.s. crystal strain in the yttria-stabilized powder (0.146(2)%; Table I) is substantially higher than that displayed by the magnesia-stabilized sintered compact (0.008(2)%; [31]), probably due to the lower annealing temperature and higher stabilizer content in the former case. The yttrium (or magnesium) content of the zirconium site (and hence the chemical formula) determined from site-occupancy refinement during Rietveld analysis is in satisfactory agreement with values obtained from empirical relationships between composition and unit cell dimension published previously [18, 35].

For T-ZrO_2 there are only minor differences between the present results for a calcined powder and those obtained earlier [31] for a sintered compact containing approximately the same amount of yttria stabilizer. The broad diffraction peaks, however, obtained from the present material, due to the small crystal size and large strain (47(1) nm and 0.127(3)%, respectively; Table I), have resulted in a lower-accuracy determination of the yttrium content of the zirconium site, relative to the values obtained by chemical analysis and from the unit cell dimensions (Table III). For the sintered compact, no such trouble was experienced (size = 160(6) nm, and strain = 0.071(2)%; [31]) so that the yttrium content from the diffraction data is in much closer agreement with the chemical and unit cell determinations.

For M-ZrO_2 the crystal structure parameters (Table IV) are essentially unchanged from those determined from shorter-wavelength neutron powder data [31] and from X-ray single-crystal data [34]. The quite low degree of crystal strain exhibited by this sample is consistent with the absence of any stabilizer cation in the structure.

Since it has been suggested that chemically pure powders (of any compound) may contain a significant fraction of amorphous surface material [38], an attempt was made to determine the crystallinity of each

TABLE IV Fractional atomic coordinates and isotropic displacement parameters for monoclinic ZrO_2

		Present work	[31]	[34]
Data type		neutron powder	neutron powder	X-ray single crystal[a]
a (nm)		0.515 26(2)	0.515 05(1)	0.5145(5)
b (nm)		0.520 77(2)	0.521 16(1)	0.520 75(5)
c (nm)		0.531 95(2)	0.531 73(1)	0.531 07(5)
β(°)		99.244(2)	99.230(1)	99.23(8)
Zr	x	0.2749(3)	0.2754(2)	0.2758(2)
	y	0.0392(3)	0.0395(2)	0.0411(2)
	z	0.2077(3)	0.2083(2)	0.2082(2)
	B/B_{eq}(nm^2)	0.0040(3)	0.0033(2)	0.0030
O1	x	0.0690(4)	0.0700(3)	0.0703(15)
	y	0.3301(3)	0.3317(3)	0.3359(14)
	z	0.3467(3)	0.3447(3)	0.3406(13)
	B/B_{eq}(nm^2)	0.0069(3)	0.0055(2)	0.0032
O2	x	0.4506(3)	0.4496(3)	0.4423(15)
	y	0.7566(4)	0.7569(3)	0.7549(14)
	z	0.4786(3)	0.4792(3)	0.4789(13)
	B/B_{eq}(nm^2)	0.0047(3)	0.0046(2)	0.0023

[a]Cell dimensions from [37]

polymorph sample, prior to the polymorph-mixture phase analyses, from neutron measurements on a 1 : 1 binary mixture of the sample with corundum. The results are shown as the first entries in Table V. For both C and T there is a small shortfall of the experimentally determined quantity of polymorph below the as-weighed quantity, corrected for impurity. This has been interpreted as a shortfall in crystallinity (and recorded in Table I), probably due to the presence of glassy intergranular phases [2, 3, 39] and/or to disorder resulting from the presence of the stabilizer cation. In the absence of neutron data recorded at different wavelengths, however, the possibility that some of the shortfall may be an artefact of extinction cannot be excluded. (As discussed briefly below, corresponding X-ray measurements were certainly affected by extinction). The M sample, with no stabilizer, shows no shortfall and can be taken to be 100% crystalline.

5.2. Phase analysis of polymorph mixtures

5.2.1. The Rietveld method

Table V gives the results of neutron phase analysis determinations performed with Equation 8 on the three binary mixtures of C and T. The agreement between the experimental and as-weighed compositions, after correction for crystallinity and the presence of impurity phases (Table I), is very satisfactory.

A corresponding analysis undertaken on the 1 : 1 C : T mixture using X-ray diffraction data provides poorer agreement between the experimental and as-weighed compositions. The linear absorption coefficients of the C, T and M phases are 65.0, 67.6 and 64.8 cm^{-1} respectively, taking account of the presence of both the yttrium stabilizer and the hafnium impurity atoms; this is not enough variation to ascribe the discrepancies in phase analyses to the effects of microabsorption. Instead, it is concluded that the lower accuracy of the method applied to X-ray data is associated with the loss of C/T peak resolution due to

TABLE V Phase analysis results (wt %) using the Rietveld and polymorph methods

Mixture	As-weighed composition		Rietveld		Polymorph
	Raw	Corrected[a]	Scale factor	Experiment[b]	Experiment[c]
C-ZrO_2	50	49.4	0.165 66(95)	46.6(5)	—
Al_2O_3	50	50.0	0.076 45(38)	50	—
T-ZrO_2	50	49.6	0.6439(39)	47.5(6)	—
Al_2O_3	50	50.0	0.073 03(37)	50	—
M-ZrO_2	50	50.0	0.1632(14)	50.2(8)	—
Al_2O_3	50	50.0	0.073 32(38)	50	—
C	25	24.5	0.1428(22)	23.7(6)	27.0
T	75	75.5	1.827(12)	76.3(12)	73.0
C	50	49.2	0.2756(24)	48.8(8)	49.4
T	50	50.8	1.154(10)	51.2(9)	50.6
C[d]	50	49.2	0.001 683(13)	57.6(11)[56.1]	u
T	50	50.8	0.004 93(5)	42.4(8) [43.9]	u
C	75	73.9	0.4448(32)	73.3(12)	78.2
T	25	26.1	0.6450(93)	26.7(6)	21.8
C	33.3	32.1	0.1756(22)	31.5(8)	35.6
T	33.3	33.2	0.7363(97)	33.1(9)	31.8
M	33.3	34.7	0.1882(25)	35.4(9)	32.6
C[d]	33.3	32.1	0.002 94(2)	29.6(4)[34.1]	u
T	33.3	33.2	0.010 95(10)	27.6(4)[35.9]	u
M	33.3	34.7	0.004 05(2)	42.8(5)[30.0]	47.2

[a]For the two-phase mixtures of C-, T- and M-ZrO_2 with Al_2O_3, the as-weighed figures are corrected to exclude the impurity phases noted in Table I. For the remaining mixtures, these figures include corrections for impurity and crystallinity (as determined from the mixtures with Al_2O_3) and are normalised so as to total 100%.

[b]Calculated from the Rietveld scale factor using Equation 8 and the ZMV values in Table I.

[c]Analysis determined with the "Polymorph Method" using either Equation 3 or 6, with the P or Q values obtained from Table VI. An entry u in this column indicates that attempts to extract the required intensities were unsuccessful.

[d]Analysis determined from X-ray powder diffraction data. Values in square brackets denote results obtained after the application of an extinction correction.

the absence of high-intensity, high-angle diffraction peaks. Neutron diffraction patterns display no such limitation because they contain large peaks at all diffraction angles.

The results of phase analyses undertaken on the 1:1:1 C:T:M ZrO_2 mixture with both neutrons and X-rays are also summarized in Table V. This assemblage mimics that found in many PSZ ceramics that have been subjected to stress and thereby contain significant quantities of M. As for the binary mixtures, the agreement between the experimental and corrected as-weighed compositions is excellent for the neutron data, but significantly poorer in the case of the X-ray data. In the latter analyses, the already poor resolution for the C/T peaks is degraded further by the presence of the M component, which is significantly overrepresented in the analysis. Similar results have been observed by other workers [19] who attributed the discrepancy to the effect of extinction in the larger crystallites in the C and T components.

It is noted that, for the same samples, extinction is more serious in X-ray than in neutron diffraction data. To further investigate the phenomenon, X-ray measurements were made on 1:1 by weight binary mixtures of the C, T and M samples with corundum. In analyses neglecting extinction, the amounts of C and T were seriously underestimated, and the amount of M underestimated slightly. The data were reanalysed using a recent version of the Rietveld refinement program LHPM7 [24] incorporating the extinction algorithm of Sabine [40]. The analyses of these binary mixtures with corundum reproduced the as-weighed compositions assuming domain sizes of 4.0, 4.3 and 1.7 μm in the C, T and M phases, respectively. When the corresponding extinction parameters were incorporated into the refinement of the X-ray data from the 1:1:1 mixture of C/T/M, the dominance of the M component disappeared, and the phase analysis was brought into much closer agreement with the as-weighed composition (see Table V again). A similar, but less marked improvement was noted for the analysis of X-ray data from the 1:1 mixture of C/T. The neutron analyses were little affected.

The above results highlight the quite dramatic influence of extinction in X-ray diffraction patterns from high symmetry materials. Its influence imposes a serious limitation on the accuracy of X-ray phase analytical work and demands attention either through the application of a specific extinction correction during the analysis, or the execution of extensive calibration experiments on "standard" materials with similar microstructure. These limitations are not severe in the case of neutron diffraction phase analysis. Further details of the extinction correction procedure, and its application to other systems, will be presented elsewhere [41].

TABLE VI Values of P and Q (calculated from Equations 4 and 7*) required for the polymorph method analysis

	P_C	P_T	Q
Neutrons (0.15 nm)	1.4600	1.4403	0.8478
X-rays (0.154056 nm)	1.2112	1.2381	0.8661

*The values of Re for Equations 4 and 7 were calculated with program LHPM7 [24], using the crystal structure models provided in Tables I to IV.

5.2.2. The polymorph method

The intensities $I(hkl)$, needed to determine X_M and X_T with Equations 2 and 5, were obtained using program LHPM7 as a simple peak fitting tool. For the determination of M, the $\{111\}$ peaks (Fig. 1) were used. In the neutron case, these were fitted as three independent Voigt functions on a linear background; in the X-ray case each was considered as an $\alpha_1:\alpha_2$ doublet. In fitting the $\{400\}$ peaks from the binary mixtures (Fig. 2), the $(400)_C$ and the $(400)_T$ were treated independently, but the $(004)_T$ was constrained to have the same width and shape as the $(400)_T$ and to lie at an angle determined by the known value (Table III) of c/a. This approach failed in the X-ray case, in that it produced a negative estimate for $I(004)_T$. For the $\{400\}$ peaks in the neutron pattern from the ternary mixture, the three required peaks and two obviously interfering monoclinic peaks were fitted simultaneously. No attempt was made to determine the $\{400\}$ intensities in the X-ray pattern from the ternary mixture. Phase abundances were calculated from X_M and X_T using Equations 3 and 6, incorporating appropriate values of P and Q from the data in Table VI. The results are shown in the final column of Table V.

The polymorph method is a rapid method for phase analysis, particularly useful for the determination of M, however, as indicated in Table V, the method fails in the difficult X-ray cases. A closer examination of the results in Table V also suggests the accuracy of the polymorph method (where applicable) tends to be poorer than that of the Rietveld method. This is in accord with expectation, since the Rietveld method includes the relative intensities of the entire diffraction patterns, rather than those of a subset of peaks. We also suggest that the Rietveld method, being essentially a single-pass technique, offers a convenience comparing favourably with that of the polymorph method in many applications.

Acknowledgements

RJH is grateful to the Foreign Office, Federal Republic of Germany, for the support of a Ludwig Leichhardt Fellowship during the course of this research. Drs E. H. Kisi and M. M. Elcombe are thanked for collecting several of the neutron diffraction data sets, and Drs B. E. Reichert, A. J. Hartshorn and M. R. Houchin kindly provided samples of phase-pure M and C/T ZrO_2, respectively.

References

1. N. CLAUSSEN, *Adv. Ceram.* **12** (1984) 325.
2. G. FISHER, *Ceram. Bull.* **65** (1986) 1355.
3. R. STEVENS, "Zirconia and Zirconia Ceramics" (Magnesium Elektron Ltd, Manchester, 1987).
4. A. H. HEUER, V. LANTERI, S. C. FARMER, R. CHAIM, R.-R. LEE, B. W. KIBBEL and R. M. DICKERSON, *J. Mater. Sci.* **24** (1989) 124.
5. H. J. ROSSELL and R. H. J. HANNINK, *Adv. Ceram.* **12** (1984) 139.
6. R. C. GARVIE, R. H. HANNINK and R. T. PASCOE, *Nature* **258** (1975) 703.
7. R. C. GARVIE and P. S. NICHOLSON, *J. Amer. Ceram. Soc.* **55** (1972) 303.
8. H. M. RIETVELD, *J. Appl. Crystallogr.* **2** (1969) 65.
9. B. D. CULLITY, "Elements of X-ray Diffraction" (Addison Wesley, Reading, Ma., 1978).
10. B. L. AVERBACH and M. COHEN, *Trans. AIME* **176** (1948) 401.
11. R. J. HILL and C. J. HOWARD, *J. Appl. Crystallogr.* **20** (1987) 467.
12. J. ADAM and B. COX, *J. Nucl. Energy*: **A, 11** (1959) 31.
13. E. D. WHITNEY, *Trans. Faraday Soc.* **61** (1965) 1991.
14. P. DUWEZ and F. ODELL, *J. Amer. Ceram. Soc.* **32** (1949) 180.
15. D. L. PORTER and A. H. HEUER, *ibid.* **62** (1979) 298.
16. H. TORAYA, M. YOSHIMURA and S. SOMIYA, *ibid.* **67** (1984) C119.
17. R. FILLIT, P. HOMERIN, J. SCHAFER, H. BRUYAS and F. THEVENOT, *J. Mater. Sci.* **22** (1987) 3566.
18. H. TORAYA, M. YOSHIMURA and S. SOMIYA, *J. Amer. Ceram. Soc.* **67** (1984) C183.
19. H. K. SCHMID, *ibid.* **70** (1987) 367.
20. P. A. EVANS, R. STEVENS and J. G. P. BINNER, *Brit. Ceram. Trans.* **83** (1984) 39.
21. H. TORAYA, *J. Appl. Crystallogr.* **19** (1986) 440.
22. H. TORAYA, *Adv. Ceram.* **21** (1987) 811.
23. A. PATERSON and R. STEVENS, *J. Mater. Res.* **1** (1986) 295.
24. R. J. HILL and C. J. HOWARD, Report No. M112, Australian Atomic Energy Commission (now ANSTO), Lucas Heights Research Laboratories, NSW, Australia (1986)
25. C. J. HOWARD, R. J. HILL and M. A. M. SUFI, *Chem. Aust.* **55** (1988) 367.
26. I. C. MADSEN and R. J. HILL, in Proceedings of the AXAA-88 Meeting: New Horizons in Analytical Science, University of Western Australia, Perth, WA, August 1988, p. 297.
27. D. L. BISH and S. A. HOWARD, *J. Appl. Crystallogr.* **21** (1988) 86.
28. R. J. HILL, C. J. HOWARD and B. E. REICHERT, *Mater. Sci. Forum* **34–36** (1988) 159.
29. C. J. HOWARD, C. J. BALL, R. L. DAVIS and M. M. ELCOMBE, *Aust. J. Phys.* **36** (1983) 507.
30. R. J. HILL, *Acta Crystallogr* **C41** (1985) 1281.
31. C. J. HOWARD, R. J. HILL and B. E. REICHERT, *ibid.* B44 (1988) 116.
32. R. A. YOUNG, E. PRINCE and R. A. SPARKS, *J. Appl. Crystallogr.* **15** (1982) 357.
33. "International Tables for X-ray Crystallography," Vol IV (Kynoch, Birmingham, 1974)
34. D. K. SMITH and H. W. NEWKIRK, *Acta Crystallogr.* **18** (1965) 983.
35. H. G. SCOTT, *J. Aust. Ceram. Soc.* **17** (1981) 16.
36. H. G. SCOTT, *J. Mater. Sci.* **10** (1975) 1527.
37. J. ADAM and M. D. ROGERS, *Acta Crystallogr.* **12** (1959) 951.
38. S. ALTREE-WILLIAMS, J. G. BYRNES and B. JORDAN, *Analyst (London)* **106** (1981) 69.
39. M. L. MECARTNEY, *J. Amer. Ceram. Soc.* **70** (1987) 54.
40. T. M. SABINE, *Acta Crystallogr.* **A44** (1988) 368, 374.
41. T. M. SABINE, C. J. HOWARD and R. J. HILL, in preparation.

Received 20 September 1989
and accepted 1 February 1990